



# Development of robust proton exchange membranes for fuel cell applications by the incorporation of sulfonated $\beta$ -cyclodextrin into crosslinked sulfonated poly(vinyl alcohol)



Balappa B. Munavalli, Satishkumar R. Naik, Mahadevappa Y. Kariduraganavar\*

Department of Studies in Chemistry, Karnatak University, Dharwad, 580 003, India

## ARTICLE INFO

### Article history:

Received 12 March 2018

Received in revised form

11 July 2018

Accepted 8 August 2018

Available online 13 August 2018

### Keywords:

Poly(vinyl alcohol)

Sulfonated  $\beta$ -cyclodextrin

Composite membrane

Proton exchange membrane

Fuel cell

## ABSTRACT

Despite significant advances in the development of proton exchange membranes for fuel cell applications, still there is a big challenge to enhance the mechanical strength and proton conductivity of the membranes to make the fuel cell technology affordable. Thus, present work describes the preparation of crosslinked sulfonated poly(vinyl alcohol) membrane using titanium glycine-*N,N*-dimethylphosphonate. It was then modified by incorporating the sulfonated  $\beta$ -cyclodextrin in different mass%. The resulting proton exchange membranes were subjected to various techniques to assess their physicochemical properties. The ion exchange capacity of the membranes was found to be in the range of 1.40 to 2.55 meq/g. The proton conductivity of the membranes was evaluated using a high precision impedance analyzer at different temperatures with 100% relative humidity. Membranes containing 16 and 20 mass% of sulfonated  $\beta$ -cyclodextrin demonstrated the excellent proton conductivity of 0.121 and 0.143 S/cm at 80 °C, respectively. The fuel cell performance study also suggests that membranes containing 16 and 20 mass% of sulfonated  $\beta$ -cyclodextrin exhibited the power density of 0.34 and 0.38 W/cm<sup>2</sup>, respectively. These values are much superior to the existing commercial Nafion<sup>®</sup> 117 membrane (9 mW/cm<sup>2</sup>). Thus, these two membranes considered as potential candidates for fuel cell applications.

© 2018 Elsevier Ltd. All rights reserved.

## 1. Introduction

The membrane based technology is being widely explored particularly for fuel cell applications. Nowadays, fuel cell technology plays an important role in automobile industries due to its easy operation, cost-effective, energy saving and eco-friendly nature. The success of fuel cell technology is primarily dependent on electrolyte membrane and its properties [1,2].

Among the different types of fuel cells, the polymer electrolyte membrane fuel cell (PEMFC) has been developed greatly for the last two decades and was successfully explored as a source of electrical power in submarines and spacecraft. In PEMFC technology, the perfluorinated sulfonic acid membrane Nafion<sup>®</sup> 117 is being used as a polymer electrolyte owing to its good chemical stability, high thermal resistance and excellent ionic conductivity. Unfortunately, this Nafion membrane has major drawbacks such as high cost and loss of conductivity at high temperatures, and thus, limits its use for wide range of applications [3–6]. To overcome these drawbacks, it

is essential to modify the existing Nafion membrane or to develop the alternative nonperfluorinated proton exchange membranes (PEM). Therefore, a sincere effort has been made recently for the development of fluorine-free alternative polymer membranes and their composites. Polymers such as polyimides [7,8], polybenzimidazole [9,10], poly(ether sulfone) [11,12], poly(aryl ether ketone) [13,14] and poly(vinyl alcohol) (PVA) [15,16] have been explored. Among these, several have been reported on PVA composite membranes, wherein polyelectrolytes were dispersed in the polymer matrices.

From literature, it is also realized that PVA based membranes are believed to be promising electrolytes for hydrogen-oxygen fuel cells owing to their low cost, excellent film forming property, super hydrophilic nature, good oxidative and hydrolytic stability. Since pure PVA membrane does not exhibit conductivity, various methods have been used to create functionalities on PVA to achieve proton conductivity [17–19]. Thus, understanding the versatility of PVA, many researchers are making their sincere efforts to develop PVA based proton exchange membranes (PEMs).

To enhance the membranes' performance, several modification methods have also been tried such as crosslinking of polymer, grafting of selective species onto an inert polymer film, and

\* Corresponding author.

E-mail address: [mahadevappayk@gmail.com](mailto:mahadevappayk@gmail.com) (M.Y. Kariduraganavar).

copolymerization and blending of PVA with relatively hydrophobic polymer [20–22]. Among these, the crosslinking method was used extensively to modulate the physicochemical properties of PVA to achieve an excellent performance for fuel cell applications. For instance, El-Toony et al. [16] developed poly(hydroxybutarate) and phosphorylated PVA membranes with different mass ratios of crosslinking agent. Among the developed membranes, the membrane containing 6 mass% of poly(hydroxybutarate) exhibited the ion exchange capacity of 1.02 meq/g with a proton conductivity of 68.9 mS/cm. Beydaghi et al. [23] prepared PVA based organic-inorganic nanocomposite membranes with nanoporous silica containing sulfonic acid groups. Among the composites, membrane containing 95 mass% of PVA and 5 mass% of SBA-15-SO<sub>3</sub>H showed an excellent water uptake of 235% with a proton conductivity of 9 mS/cm. Using electrospinning technique and solvent casting techniques, Boonpoo-nga et al. [24] developed the fibers of PVA by varying the mass% of poly(styrene sulphonic acid-co-maleic acid) and imidazole. They found that proton conductivity of the solvent-cast membrane was slightly higher than those of fibres developed by electrospinning technique. A maximum proton conductivity of 121  $\mu$ S/cm was achieved from the solvent-cast membrane at 200 °C. Boroglu et al. [25] synthesized the proton conducting polymer membranes with PVA and diamine-containing organic molecules. Among the synthesized membranes, PVA membrane containing 20 mass% of 4,4'-diaminodiphenyl ether-2,2'-disulfonic acid exhibited proton conductivity of 16.53 mS/cm. Liu et al. [18] reported the blend membranes of PVA/hexafluoroglutaric acid (HFA) with benzenesulfonic acid sodium salt. The PVA/HFA (2/2) membrane showed ion exchange capacity of 1.043 meq/g with a proton conductivity of 56.3 S/cm before 60 °C. After 60 °C, both ion exchange capacity and proton conductivity were changed to 1.158 meq/g and 62.7 mS/cm, respectively. The sulfonated PVA membranes with dual crosslinkers were synthesized by Tseng and others [26]. Among these membranes, the membrane of sulfonated PVA (97%)/4,4'-oxydiphthalic anhydride (1.5%)/epoxy (1.5%) exhibited the proton conductivity of 218 mS/cm at 70 °C. Erkartal et al. [27] reported the PVA based composite membranes with poly(2-acrylamido-2-methylpropane sulfonic acid) and 1,2,4-triazole and obtained the highest proton conductivity of 2 mS/cm at 150 °C among the membranes developed.

Recently, an effort was also made to assess the efficiency of the PVA based membranes for fuel cell applications by determining the power density at different temperatures. For instance, Yang et al. [28] prepared the composite membranes made of sulfonated poly(ether ether ketone) and sulfated PVA. Among the membranes developed, membrane containing 75 mass% of sulfated PVA exhibited the power density of 23.32 mW/cm<sup>2</sup> with an open circuit voltage (OCV) value of 0.625 V at 80 °C. Similarly, Higa et al. [29] reported the modification of crosslinked PVA membrane with 2-methyl-1-propanesulfonic acid (AMPS). Among these, membranes with 2 mol% of AMPS annealed at 190 °C showed the power density of 2.4 mW/cm<sup>2</sup> with an open circuit voltage of 0.54 V at 25 °C.

Understanding the versatility of PVA in aforementioned studies, we have synthesized the crosslinked sulfonated PVA membrane. This membrane was further modified by incorporating the sulfonated  $\beta$ -cyclodextrin ( $\beta$ -CD) in different mass ratios with a prime aim to improve proton conductivity, mechanical strength and thermal stability. The titanium glycine-*N,N*-dimethylphosphonate (TGDMP) was used as a crosslinking agent to control the dimensional stability of the membranes. The proton conductivity was also enhanced owing to the presence of negatively charged carboxylic groups in TGDMP. The physicochemical changes in the resulting membranes were systematically investigated using Fourier transform infrared spectrometer, wide-angle X-ray diffractometer, thermogravimetric analyzer, differential scanning calorimeter and

scanning electron microscope. The mechanical properties of the membranes were evaluated using a universal testing machine. The water uptake, swelling ratio, chemical stability, ion exchange capacity and proton conductivity were determined. The fuel cell performance was assessed using a fuel cell workstation. At the end, a short term durability test was also performed for the selective membranes at a fixed current density. The results were discussed in terms of molecular structures of the membranes.

## 2. Experimental

### 2.1. Materials

Poly(vinyl alcohol) ( $M_w$  ~125,000; 87.5% hydrolyzed), 1,4-butane sultone and  $\beta$ -cyclodextrin were procured from Sigma-Aldrich Chemicals, USA. Titanium chloride (TiCl<sub>4</sub>), toluene and phosphorus oxide (P<sub>2</sub>O<sub>5</sub>) were purchased from Spectrochem Pvt. Ltd., Mumbai, India. *N,N*-Bis(phosphonomethyl)-glycine was synthesized according to the procedure reported [30]. Hydrochloric acid, acetic acid, sulfuric acid, calcium carbonate (CaCO<sub>3</sub>), sodium carbonate (Na<sub>2</sub>CO<sub>3</sub>), sodium hydride (NaH), acetone and ethanol were purchased from S. D. Fine Chemicals Ltd., Mumbai, India. All the chemicals were of reagent grade and used without further purification. Double distilled water was used throughout the work.

### 2.2. Preparation of titanium glycine-*N,N*-dimethylphosphonate (TGDMP)

The TGDMP was synthesized according to the procedure reported by Kariduraganavar and his group [31]. Briefly, hydrochloric acid (2 M; 430 mL) containing 0.3 M of TiCl<sub>4</sub> was added portionwise while stirring into *N,N*-bis(phosphonomethyl)-glycine (0.63 M; 400 mL) solution. After 24 h, the precipitate thus formed was filtered and washed with distilled water until the pH of the filtrate was in between 3 and 3.5, and then it was dried over P<sub>2</sub>O<sub>5</sub>. The size of the particles was determined using zeta-sizer (Horiba Scientific, SZ-100, Japan) at 25 °C by dispersing the TGDMP in deionized water and data are presented in Fig. 1. It is noticed that size of the particles in a narrow range and the average diameter was found to be 2  $\mu$ m.

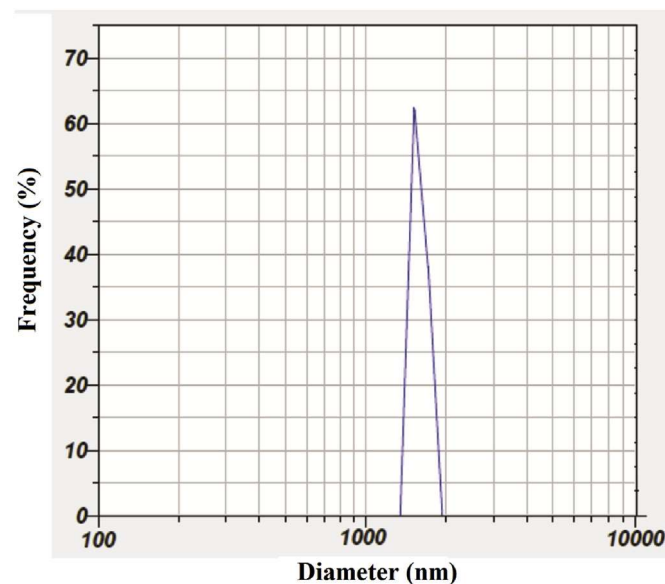


Fig. 1. The size of TGDMP particles.

### 2.3. Preparation of sulfonated $\beta$ -cyclodextrin

Fig. 2 shows the sulfonation reaction of  $\beta$ -CD. The sulfonated  $\beta$ -CD was prepared using the commercially available  $\beta$ -CD. Briefly, the  $\beta$ -cyclodextrin was initially sulfonated with 90% sulfuric acid while maintaining the temperature between 0 and 5 °C for 2 h. The resulting superfluous sulfuric acid was treated with  $\text{CaCO}_3$  and filtered. To the filtrate, alcohol was added portionwise while stirring and kept overnight below 5 °C. The sedimentation thus formed on the upper layer was slowly removed and pH of the solution was adjusted to 10.5 by adding dilute  $\text{Na}_2\text{CO}_3$  solution. After two hours, pH of the solution was brought to 7.0 by adding acetic acid dropwise and filtered. To the filtrate, the sufficient quantity of alcohol was added to form the precipitate. The white precipitate thus formed was washed with acetone and followed by ether. The white powder was finally dried in a vacuum oven at 110 °C.

### 2.4. Preparation of sulfonated poly(vinyl alcohol)

The sulfonated PVA was synthesized in a two-step reaction. In the first step, PVA (20 g) was added to 1000 mL capacity round bottom flask containing 500 mL of ethanol. To this, sodium hydride (10.6 g) was added slowly with constant stirring followed by an addition of butane sultone (8 g). The reaction temperature was raised from ambient to 80 °C and kept for 10 h. In the second step, the terminated Na was replaced with H by pouring the resultant solution into 50% HCl solution. The precipitate thus formed was filtered and washed several times with ethanol. The resulting sulfonated PVA powder was dried for 6 h in a vacuum oven at 50 °C. The sulfonation process of PVA is shown in Fig. 3.

### 2.5. Preparation of crosslinked sulfonated PVA and its composite membranes

The sulfonated PVA (4 g) was dissolved at room temperature in 100 mL of distilled water with constant stirring for about 24 h and then filtered. To this filtrate, a known amount of TGDMP was added and stirred at 120 °C for 5 h. The resulting homogeneous solution was spread onto a clean glass plate with the aid of a casting knife in a dust-free atmosphere. It was then allowed to dry at ambient temperature for about 2–3 days. The completely dried membrane was subsequently peeled-off and was designated as SPT. The same

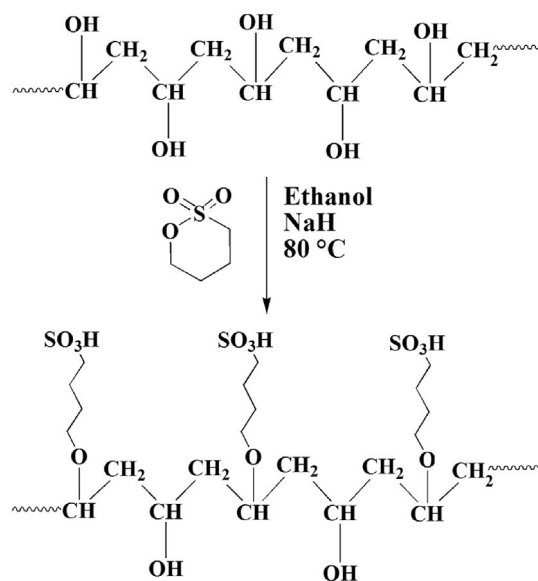


Fig. 3. Synthesis of sulfonated poly(vinyl alcohol).

procedure was followed for the preparation of composite membranes. However, the amount of sulfonated  $\beta$ -CD with respect to SPT was varied as 4, 8, 12, 16 and 20 mass%, and the resulting membranes were designated as SPTC-1, SPTC-2, SPTC-3, SPTC-4 and SPTC-5, respectively. The higher amount of sulfonated  $\beta$ -CD beyond 20 mass% was also tried, but failed to get good membrane, and thus it was restricted to 20 mass% of sulfonated  $\beta$ -CD. The preparation scheme of SPT and its composite membranes is shown in Fig. 4. The thickness of the resulting membranes was measured at different points using a Peacock dial thickness gauge (Model G, Ozaki MFG Co. Ltd., Japan) with an accuracy of  $\pm 2 \mu\text{m}$ . The thickness of the membranes was found to be  $85 \pm 2 \mu\text{m}$ .

### 2.6. Membrane characterization

#### 2.6.1. Fourier transform infrared (FTIR) spectroscopy

The sulfonation of both PVA and  $\beta$ -CD, crosslinking of sulfonated PVA and the incorporation of  $\beta$ -CD into crosslinked sulfonated PVA

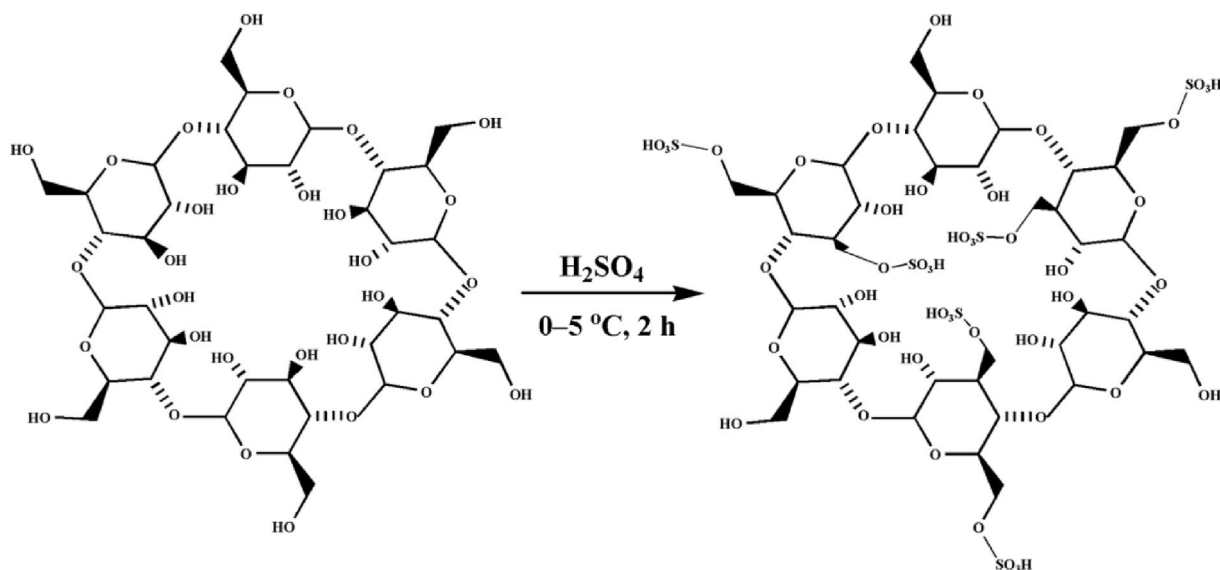


Fig. 2. Synthesis of sulfonated  $\beta$ -cyclodextrin.

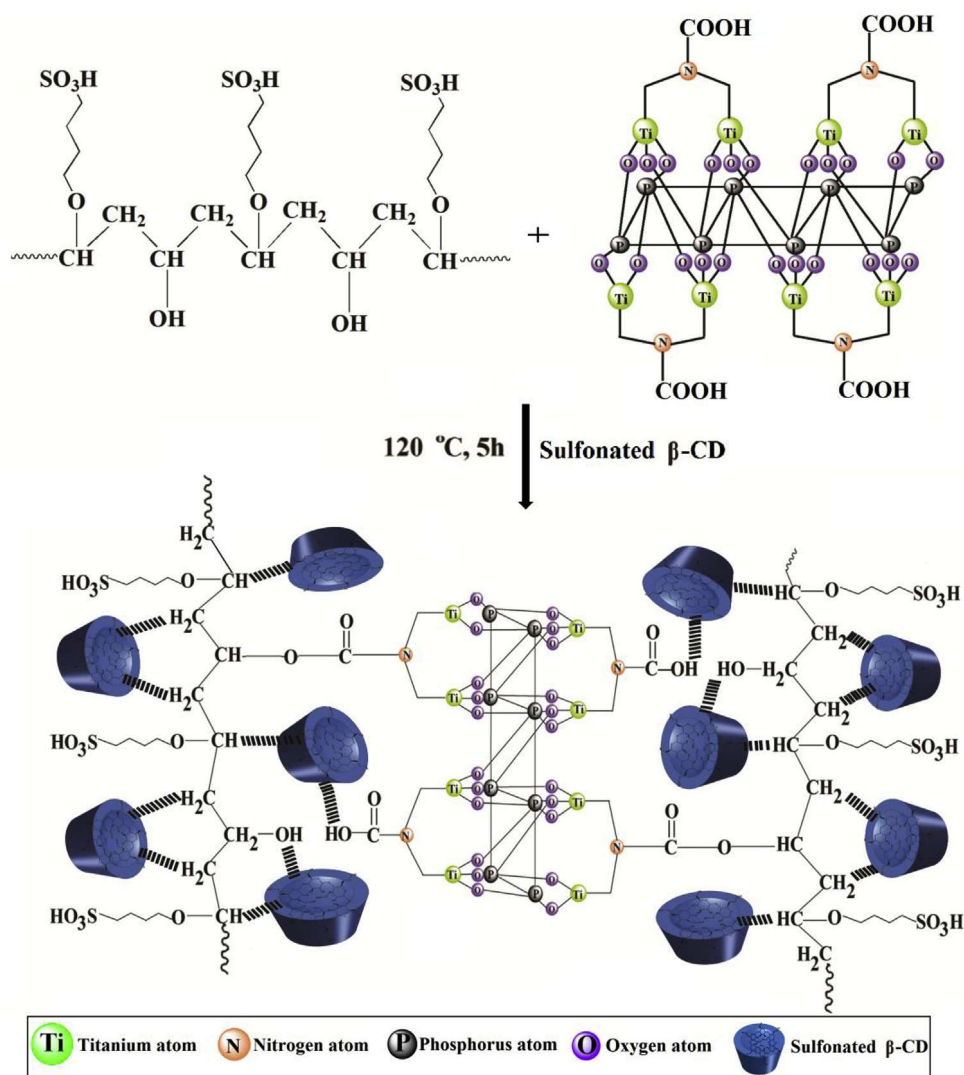


Fig. 4. Synthesis of TGDMP crosslinked sulfonated PVA and its composite membranes.

membrane were confirmed by FT-IR spectrometer (Model Nicolet, Impact-410, Thermo Fisher Scientific, USA). Membrane samples were ground well to make KBr pellets under a hydraulic pressure of 600 kg/cm<sup>2</sup> and the spectra were recorded in the range of 500–4000 cm<sup>-1</sup>. In order to estimate the changes in the intensities of the characteristic bands with respect to the amount of  $\beta$ -CD, the weights of membrane sample and KBr were kept constant.

#### 2.6.2. Wide-angle X-ray diffraction (WAXD)

To study the effect of  $\beta$ -CD content on the morphology of crosslinked sulfonated PVA membrane, all the membranes were subjected to wide-angle X-ray diffractometer (Model D-8 advanced, Bruker's, USA). The source of X-ray was Ni-filtered CuK $\alpha$  radiation. The diffraction patterns were recorded in the reflection mode at an angle  $2\theta$  over a range of 10–50° at a constant speed of 8°/min.

#### 2.6.3. Thermogravimetric analysis (TGA)

Thermal stability of the crosslinked sulfonated PVA and its composite membranes was investigated using thermogravimetric analyzer (Model SDT Q600, TA Instruments, Perkin-Elmer TGA/DTA thermogravimetric analyzer, USA). The weight of the samples employed for each record was about 8 to 10 mg and heated from

ambient to 900 °C at a heating rate of 10 °C/min under nitrogen atmosphere.

#### 2.6.4. Differential scanning calorimetry (DSC)

Differential thermograms of the crosslinked sulfonated PVA and its composite membranes were measured using differential scanning calorimeter (Model DSC Q20, TA Instruments, USA). Sample weights ranged from 8 to 10 mg and heated from ambient to 400 °C at a heating rate of 10 °C/min under nitrogen atmosphere.

#### 2.6.5. Scanning electron microscopy (SEM)

Surface and cross-section views of the crosslinked sulfonated PVA and its composite membranes were examined using scanning electron microscope (Model JSM-400 Å, JEOL, Japan). Before scanning, all the samples were dried in a vacuum chamber and coated with a conductive layer (400 Å) of sputtered gold.

#### 2.6.6. Mechanical properties

Mechanical properties of the developed membranes were measured using universal testing machine (UTM) by ASTM D638 method (Model LR5K, Lloyd Instruments Ltd., UK). Dumb-bell shaped specimens were prepared using the ASTM standard D638.

The test was carried out at 30 °C with 80% relative humidity (RH) using a gauge length and a cross head speed of 15 mm and 2 mm min<sup>-1</sup>, respectively.

### 2.6.7. Oxidative and hydrolytic stability

The membrane samples of uniform size were soaked in Fenton's reagent (3% H<sub>2</sub>O<sub>2</sub> and 2 ppm FeSO<sub>4</sub>) at 80 °C. The oxidative stability was evaluated by recording the percent of the remaining weight (RW%) and change in the IEC. However, the hydrolytic stability of the membranes was evaluated by immersing the membranes in water at 100 °C in a pressurized closed reactor for 10 h under humidified condition.

### 2.6.8. Water uptake and swelling ratio

The water uptake of the crosslinked sulfonated PVA and its composite membranes was studied between the temperature range of 25 and 80 °C by recording the change in weight between the dried and hydrated states. The membranes were first dried at 110 °C in a vacuum oven till constant weights attained. The dried membranes were then immersed in water at different temperatures for 24 h to attain the equilibrium of water absorption. The swollen membranes were removed and weighed as quickly as possible after careful blotting with a tissue paper on a digital microbalance (Model B204–S, Mettler-Toledo International, Switzerland) with an accuracy of ±0.01 mg. The experiments were performed at least three times and the results were averaged. The water uptake (WU) was determined using Eq. (1):

$$\text{Water Uptake (\%)} = \frac{W_{\text{wet}} - W_{\text{dry}}}{W_{\text{dry}}} \times 100 \quad (1)$$

where  $W_{\text{wet}}$  and  $W_{\text{dry}}$  are the mass of wet and dry membranes, respectively. The dimensional stability of the membranes was arrived by immersing the sample in water at various temperatures for 24 h. The change in the length and thickness was calculated using Eqs. (2) and (3):

$$\text{Swelling Ratio (\%)} = \frac{L_{\text{wet}} - L_{\text{dry}}}{L_{\text{dry}}} \times 100 \quad (2)$$

$$\text{Swelling Ratio (\%)} = \frac{D_{\text{wet}} - D_{\text{dry}}}{D_{\text{dry}}} \times 100 \quad (3)$$

where  $L_{\text{wet}}$  and  $L_{\text{dry}}$  are the lengths of wet and dry membranes, respectively. Similarly,  $D_{\text{wet}}$  and  $D_{\text{dry}}$  are the respective thicknesses of wet and dry membranes.

### 2.6.9. Ion exchange capacity (IEC)

The ion exchange capacity of the crosslinked sulfonated PVA and its composite membranes was determined by a back titration method. A piece of dried protonated membranes was weighed and equilibrated by immersing in 2 M NaCl solution for 24 h to exchange the protons of sulfonic acid groups with sodium ions. The concentration of HCl was determined from the release of H<sup>+</sup> ions from the membrane sample by titrating with 0.01 M NaOH solution. The ion exchange capacity was calculated using Eq. (4):

$$\text{IEC (meq/g)} = \frac{\Delta V_{\text{NaOH}} \times C_{\text{NaOH}}}{W_s} \quad (4)$$

where  $\Delta V_{\text{NaOH}}$ , the volume of NaOH solution consumed;  $C_{\text{NaOH}}$ , the concentration of NaOH solution; and  $W_s$  is the weight of membrane sample. Since, the ion exchange capacity largely depends on degree of sulfonation, it was prompted us to calculate the degree of

sulfonation (DS) of the resulting sulfonated PVA membrane using Eq. (5).

$$\text{DS(\%)} = \frac{\text{IEC} \times \text{Molecular weight of monomer unit of polymer}}{100 - (\text{IEC} \times \text{Molecular weight of sulfonic acid group})} \times 100 \quad (5)$$

### 2.6.10. Proton conductivity

The proton conductivity of the membranes was measured using high precision impedance analyzer (Model HIOKI-IM 3570, HIOKI E.E. Corporation, Japan) in the frequency range of 4 Hz–5 MHz. Membrane sample with a dimension of 2 cm × 1 cm was placed between the two stainless steel electrodes. The proton conductivity of the samples was measured in a longitudinal direction between the temperature range of 25 and 80 °C at 100% relative humidity (RH) and also by varying the humidity at 80 °C. From the impedance data, the proton conductivity (S) of the samples was calculated using Eq. (6):

$$S(\text{S/cm}) = \frac{L}{R \times A} \quad (6)$$

where  $L$  is the distance between the electrodes (cm);  $A$ , is the surface area required for a proton to penetrate the membrane (cm<sup>2</sup>), and  $R$  is the resistance obtained from the low intersection of the high-frequency semicircle on a complex impedance plane with Z axis.

### 2.6.11. Fuel cell performance and durability

The single cell performance of the membranes was evaluated using a membrane electrode assembly (MEA) in fuel cell workstation (Fuel Cell Technologies, Inc. USA). The commercially available carbon cloth as a gas diffusion layer, 40 wt% of Pt/C (0.4 mg Pt/cm<sup>2</sup>) as a catalyst and Nafion as a binder were used for the fabrication of MEA. A serpentine flow-pattern of graphite blocks was used as a current collector. The electrodes were applied as cathode and anode by interposing the MEA. The effective area of the membrane in MEA was 5 cm<sup>2</sup>. The gases (H<sub>2</sub> and O<sub>2</sub>) were humidified using gas humidity chambers set at 80 °C. The cell performance was evaluated at 80 °C between 0.2 and 1.0 V by purging hydrogen (250 cm<sup>3</sup>/min) and oxygen (600 cm<sup>3</sup>/min) gases to anode and cathode, respectively. Similarly, the membranes' durability test was performed at 80 °C with 30% relative humidity at fixed current density of 0.2 A/cm<sup>2</sup> for 100 h.

## 3. Results and discussion

### 3.1. Fourier transform infrared spectroscopy

Fig. 5a illustrates the FTIR spectra of TGDMP, sulfonated β-CD, sulfonated PVA and TGDMP crosslinked sulfonated PVA. In the TGDMP spectrum, a strong and broad band appeared at around 3400 cm<sup>-1</sup>, which corresponds to the hydroxyl groups. The bands appeared at 1735 and 1638 cm<sup>-1</sup> are respectively assigned to –COOH and –COO<sup>-</sup> stretching vibrations. The multiple bands observed in the range of 1000–1200 cm<sup>-1</sup> are the characteristic bands of phosphate groups. A weak band that appeared at 612 cm<sup>-1</sup> was attributed to the deformation vibration of Ti–O bond. All these bands are in good agreement with the earlier reports [30,31].

The spectrum of sulfonated β-CD displayed a broad –OH stretching band at around 3400 cm<sup>-1</sup>. The band appeared at 2834 cm<sup>-1</sup> could be attributed to asymmetric –CH<sub>2</sub> stretching

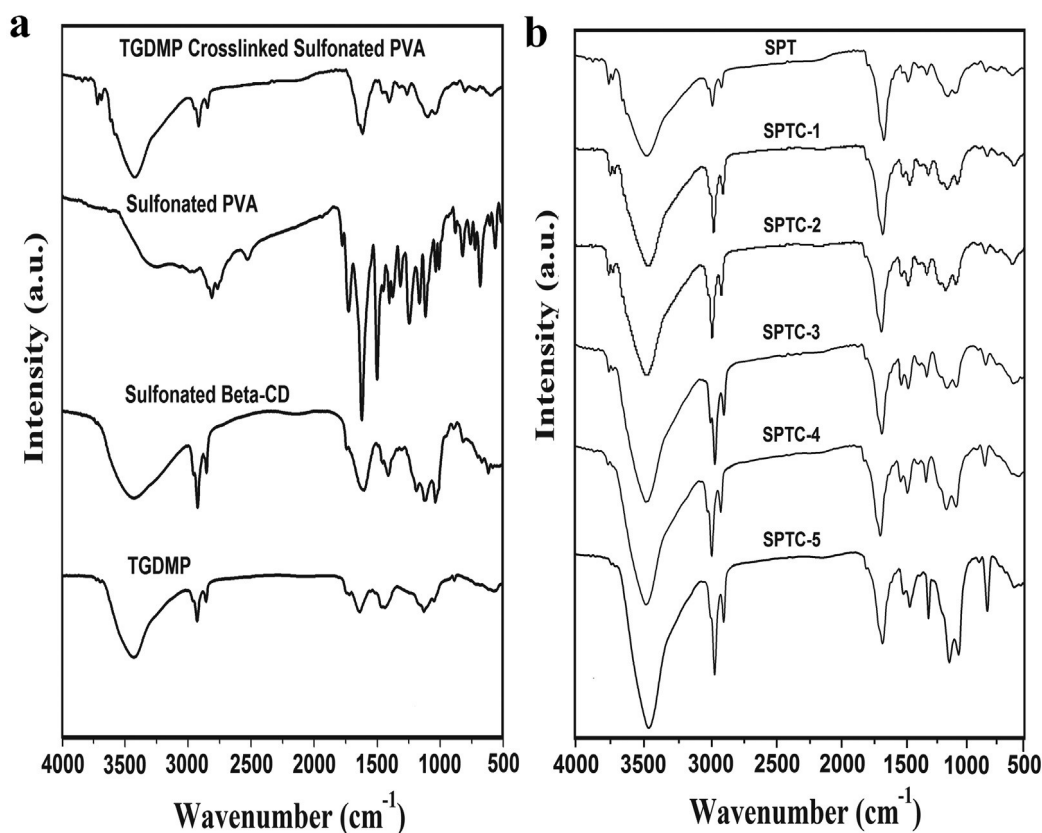


**Fig. 5.** a. The infrared spectra of (a) TGDMP, sulfonated  $\beta$ -CD, sulfonated PVA and TGDMP crosslinked sulfonated PVA; and (b) crosslinked sulfonated PVA (SPT) and its sulfonated  $\beta$ -CD incorporated composite membranes (SPTC-1 to SPTC-5).

vibrations. The bands appeared between 1000 and 1200  $\text{cm}^{-1}$  correspond to C–O stretching vibration. Similarly, the bands appeared at 689, 993 and 1100  $\text{cm}^{-1}$  are respectively attributed to S–O stretching vibrations of sulfonic acid groups, symmetric and asymmetric stretchings of  $\text{SO}_3$  groups. All these bands ascertain the successful sulfonation of  $\beta$ -CD.

The spectrum of sulfonated PVA exhibited a broad band observed at 3294  $\text{cm}^{-1}$ , and this was assigned to both hydroxyl and  $-\text{SO}_3\text{H}$  groups of functionalized PVA. A small band at 1720  $\text{cm}^{-1}$  was observed and was attributed to the presence of residual vinyl acetate groups in 99.5% hydrolyzed PVA. The bands appeared between 1000 and 1200  $\text{cm}^{-1}$  were assigned to symmetric stretching vibrations of sulfonic groups. The C–O band also appeared almost at the same frequency of  $\text{SO}_3$  groups. These evidences clearly support the successful sulfonation of PVA.

Upon introducing TGDMP as crosslinker in sulfonated PVA membrane matrix, the characteristic bands of sulfonated PVA appeared at 3294, 2834 and 1427  $\text{cm}^{-1}$  were shifted to 3480, 2920 and 1520  $\text{cm}^{-1}$ , respectively. These were respectively assigned to the stretching vibrations of hydroxyl groups, C–H stretching and C–H bending of sulfonated PVA. This is attributed to enhanced hydrogen bonding and electrostatic interaction between the sulfonated PVA and TGDMP. This indicates that there is a good compatibility between the sulfonated PVA and TGDMP. Similar conclusions were made in the paper reported by Kariduraganavar and his group [31].

Fig. 5b illustrates the FTIR spectra of crosslinked sulfonated PVA (SPT) and its  $\beta$ -cyclodextrin incorporated composite membranes (SPTC-1 to SPTC-5). A characteristic strong and broad band was observed at around 3400  $\text{cm}^{-1}$  in all the membranes, which

corresponds to stretching vibrations of hydroxyl and sulfonated groups of PVA. The multiple bands appeared between 1000 and 1200  $\text{cm}^{-1}$  were assigned to both C–O and S–O stretchings. The band observed at 830  $\text{cm}^{-1}$  signifies the existence of S–O stretching vibrations in the  $\text{SO}_3\text{H}$  groups. The intensities of all these bands were correspondingly increased with increasing the mass% of sulfonated  $\beta$ -CD. All these spectral evidences clearly show that the sulfonated  $\beta$ -CD was successfully incorporated into crosslinked sulfonated PVA and support the formation of composite membranes.

### 3.2. Wide-angle X-ray diffraction

To study the effect of sulfonated  $\beta$ -CD content on the membrane morphology of crosslinked sulfonated PVA, the wide-angle X-ray diffraction study was performed and the patterns thus obtained are presented in Fig. 6. Generally, when polymer is dominated with crystalline domains, the diffraction peaks of such polymer are sharp [32]. From the patterns, it is observed that diffraction pattern of crosslinked sulfonated PVA membrane exhibited a typical peak at  $2\theta = 20^\circ$  and was assigned to a mixture of (101) and (200) crystalline planes. As the content of sulfonated  $\beta$ -CD was incorporated into crosslinked sulfonated PVA, the intensity of the peak appeared at  $2\theta = 20^\circ$  was increased remarkably as can be seen clearly in the XRD pattern of SPTC-1. This is because of the increased crystalline domains in crosslinked sulfonated PVA membrane. This crystallinity is mainly due to the presence of free  $-\text{OH}$  groups in PVA chain as well as in  $\beta$ -CD. These groups underwent dehydration during the annealing process and thereby the crosslinking density was greatly enhanced. However, the intensity of this peak was increased

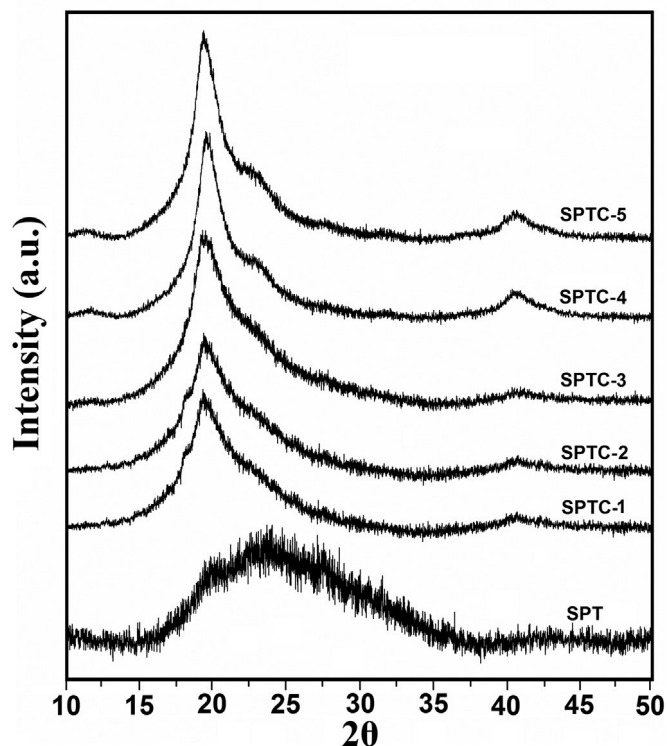


Fig. 6. Wide-angle X-ray diffraction patterns of crosslinked sulfonated PVA (SPT) and its sulfonated  $\beta$ -CD incorporated composite membranes (SPTC-1 to SPTC-5).

correspondingly with increasing the mass% of sulfonated  $\beta$ -CD as can be seen from the patterns of SPTC-2 to SPTC-5. This suggests that crystalline domain was greatly increased and thereby both thermal and mechanical properties of the membranes were correspondingly increased.

### 3.3. Thermogravimetric analysis

Thermal stability of the crosslinked sulfonated PVA and its composite membranes was analyzed using thermo-gravimetric analysis and the resulting thermograms are shown in Fig. 7. It is observed that all the membranes were thermally stable up to 145 °C and apparently no weight loss was observed, indicating that membranes have sufficiently high thermal stability. Upon increasing the mass% of sulfonated  $\beta$ -CD in the crosslinked sulfonated PVA, the thermal stability of SPTC-1 to SPTC-5 membranes was gradually increased. This is expected owing to increased crystalline domains in the membrane matrix as clearly supported from the WAXD patterns. From the thermograms, it is also observed that all the membranes underwent degradation in two stages. The first weight loss occurred between 145 and 380 °C, which correspond to the decomposition of sulfonated  $\beta$ -CD. The second weight loss was observed in the range of 380–740 °C, which was attributed to the degradation of crosslinked sulfonated PVA chain. From these TGA thermograms, it is also observed that the membranes' residual amounts were increased with increasing the sulfonated  $\beta$ -CD content. This explicitly says that the thermal stability of membranes was enhanced with increasing the mass% of sulfonated  $\beta$ -CD.

### 3.4. Differential scanning calorimetry

DSC is a widely used analytical tool to understand the thermal

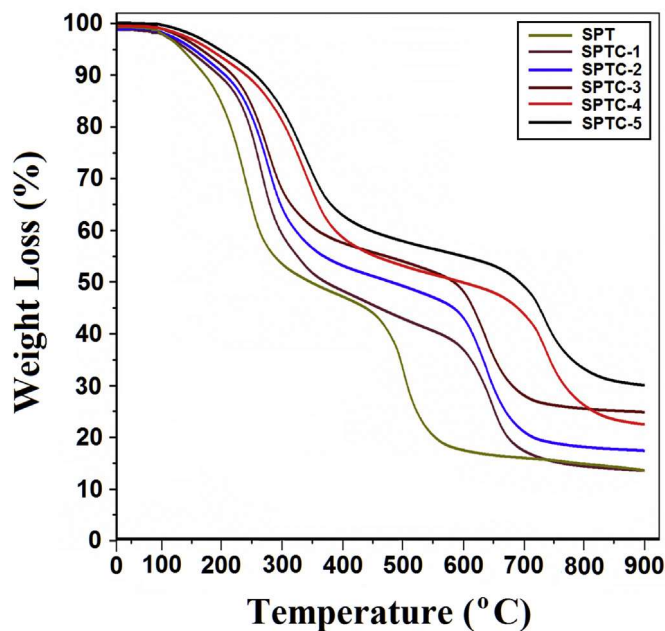


Fig. 7. TGA curves of crosslinked sulfonated PVA (SPT) and its sulfonated  $\beta$ -CD incorporated composite membranes (SPTC-1 to SPTC-5).

behavior of polymers. Accordingly, all the developed membranes were subjected to DSC and the resulting thermograms are presented in Fig. 8 and data are presented in Table 1. The crosslinked sulfonated PVA membrane (SPT) exhibited  $T_g$  and  $T_m$  at 85 and 175 °C, respectively. These were correspondingly increased from 85

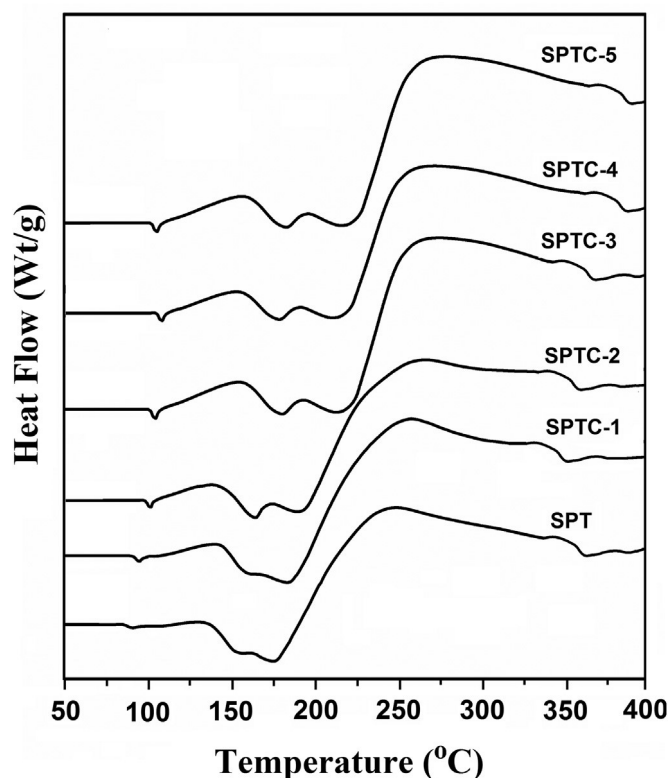


Fig. 8. DSC curves of crosslinked sulfonated PVA (SPT) and its sulfonated  $\beta$ -CD incorporated composite membranes (SPTC-1 to SPTC-5).

to 107 °C, and 175–239 °C by the incorporation of sulfonated  $\beta$ -CD and with the increase of its mass%. This is mainly because of the decreased free-volume and the establishments of number of hydrogen bonding in the crosslinked sulfonated PVA matrix. These two parameters are responsible for increasing the degree of crystallinity in the resulting membranes, and thereby the thermal property of membranes was increased. This is also well supported from the WAXD and TGA data.

### 3.5. Scanning electron microscopy

The morphology of the crosslinked sulfonated PVA and its sulfonated  $\beta$ -CD incorporated composite membranes was examined using scanning electron microscope and the resulting surface and cross-section views are presented in Fig. 9. From the images, it is observed that surface morphology of the membranes (SPT to SPTC-4) was smooth and no apparent clusterings on the surface of the membranes. This clearly supported from the cross-section views of the corresponding membranes. However, when 20 mass% sulfonated  $\beta$ -CD was incorporated into crosslinked sulfonated PVA (SPTC-5), the crystal domains were noticed on the surface of the membrane. This is reflected in its cross-section view also. This might be due to incompatibility that occurred between the crosslinked sulfonated PVA and sulfonated  $\beta$ -CD. This was fully supported from the WAXD patterns, and thus the incorporation of sulfonated  $\beta$ -CD was restricted to only 20 mass% during the preparation of composite membranes.

### 3.6. Mechanical properties

Tensile strength and elongation at break of a membrane often determine its suitability for PEMFC applications. To demonstrate the effect of TGDMP and sulfonated  $\beta$ -CD on the mechanical properties of the sulfonated PVA membrane, we have measured the tensile strength, elongation at break and Young's modulus of the TGDMP crosslinked sulfonated PVA and its sulfonated  $\beta$ -CD incorporated composite membranes and the data are presented in Table 1. The stress-strain curves of the crosslinked sulfonated PVA and its composite membranes are shown in Fig. 10. The membrane SPT showed a lower mechanical strength (52.44 MPa) while exhibiting a better elongation (26.21%). The membranes particularly of SPTC-4 and SPTC-5 showed excellent tensile strength of 81.34 and 97.22 MPa with elongation at break of 15.28 and 11.40%, respectively. From the data, it is also observed that the tensile strength of the membranes was increased significantly with increasing the mass% of sulfonated  $\beta$ -CD. This is expected, since the hydroxyl groups of  $\beta$ -CD undergo hydrogen bonding with the crosslinked sulfonated PVA. As a result, the reduction of free-volume and the hindrance of chain mobility in the membrane matrix obviously increase the tensile strength. This clearly suggests that the crosslinking moiety of TGDMP and sulfonated  $\beta$ -CD greatly enhanced the mechanical properties of the membranes.

### 3.7. Oxidative and hydrolytic stabilities

The oxidative stability of proton exchange membranes is very important property to understand their practical utility for fuel cell applications. During the operation of fuel cell, the PEMs are known to undergo degradation resulting from the hydroxyl or peroxy free radicals formed by the decomposition of  $H_2O_2$  at the cathode [36]. The oxidative stability of the membranes was evaluated in Fenton's reagent at 80 °C and the results are presented in Table 2. It can be seen that the crosslinked sulfonated PVA membrane was ruptured after 22 h and showed 96.4% of residue weight. However, the membranes with higher mass% of sulfonated  $\beta$ -CD (4–20 mass%) were stable up to 17 h and showed slightly higher weight loss as compared to crosslinked sulfonated PVA. The crosslinked membrane showed a minimum loss of IEC as compared to composite membranes. This is due to increased hydrophilicity of the composite membranes and thereby free radicals mainly occur in or near the hydrophilic domains. This implies that owing to the presence of crosslinking groups in PVA matrix restricted the free radicals to reach the polymer main chain, and thereby greatly suppressed the oxidative degradation of polymer backbone. Similarly, all the membranes were soaked in water at 100 °C for 10 h to evaluate their hydrolytic stability. It is found that all the membranes retained more than 93% of their original weight and apparently no change was noticed in regard to their shape and appearance after the treatment. This suggests that the chemical structure of the membranes was protected by the crosslinking groups of TGDMP against the hydrolytic degradation during the process.

### 3.8. Water uptake and swelling ratio

The water uptake and swelling ratio of the membranes were measured at different temperatures under immersed conditions in deionized water and the results are presented in Figs. 11 and 12, respectively. The data are presented in Table 3. From the data, it is observed that the water uptake was increased from 42 to 67% at 25 °C and 58 to 79% at 80 °C by the incorporation of sulfonated  $\beta$ -CD and increase of its mass% in SPT membrane. This is mainly due to increase of hydrophilic domains such as sulfonic and hydroxyl groups in the membranes. Generally, a higher sulfonation level leads to a better water uptake and in turn results to a greater IEC value. Based on the results, we conclude that the introduction of sulfonated  $\beta$ -CD in TGDMP crosslinked sulfonated PVA was greatly contributed for the overall increase of water uptake. However, the hydrophobic region greatly suppresses the water uptake. This process is predominant when the hydrophobic region is dominant, but it is equally important so as to retain the mechanical strength of the membrane. In present study, the branched sulfonic acid groups which are chemically bonded to both PVA and  $\beta$ -CD could allow the water into the hydrophobic region, which in turn contribute to higher water uptake in the resulting composite membranes.

On the other hand, the high swelling ratio of the membranes is

**Table 1**  
Thermal and mechanical properties of TGDMP crosslinked sulfonated PVA and its composite membranes.

Membranes	$T_g$ (°C)	$T_m$ (°C)	Young's modulus (MPa)	Tensile strength (MPa)	Elongation at break (%)
SPT	85	175	1845 $\pm$ 6	52.44 $\pm$ 0.32	26.21 $\pm$ 0.29
SPTC-1	89	178	1936 $\pm$ 7	60.94 $\pm$ 0.21	24.90 $\pm$ 0.58
SPTC2	93	192	2045 $\pm$ 5	65.52 $\pm$ 0.54	20.45 $\pm$ 0.65
SPTC-3	97	222	2367 $\pm$ 3	74.13 $\pm$ 0.41	18.14 $\pm$ 0.42
SPTC-4	103	230	2275 $\pm$ 6	81.34 $\pm$ 0.21	15.28 $\pm$ 0.57
SPTC-5	107	239	2351 $\pm$ 5	97.22 $\pm$ 0.36	11.40 $\pm$ 0.36
Nafion <sup>®</sup> 117 <sup>a</sup>	132	207–249	–	27.00	220

<sup>a</sup> Data of Nafion<sup>®</sup> 117 are collected from Refs. [33–35].



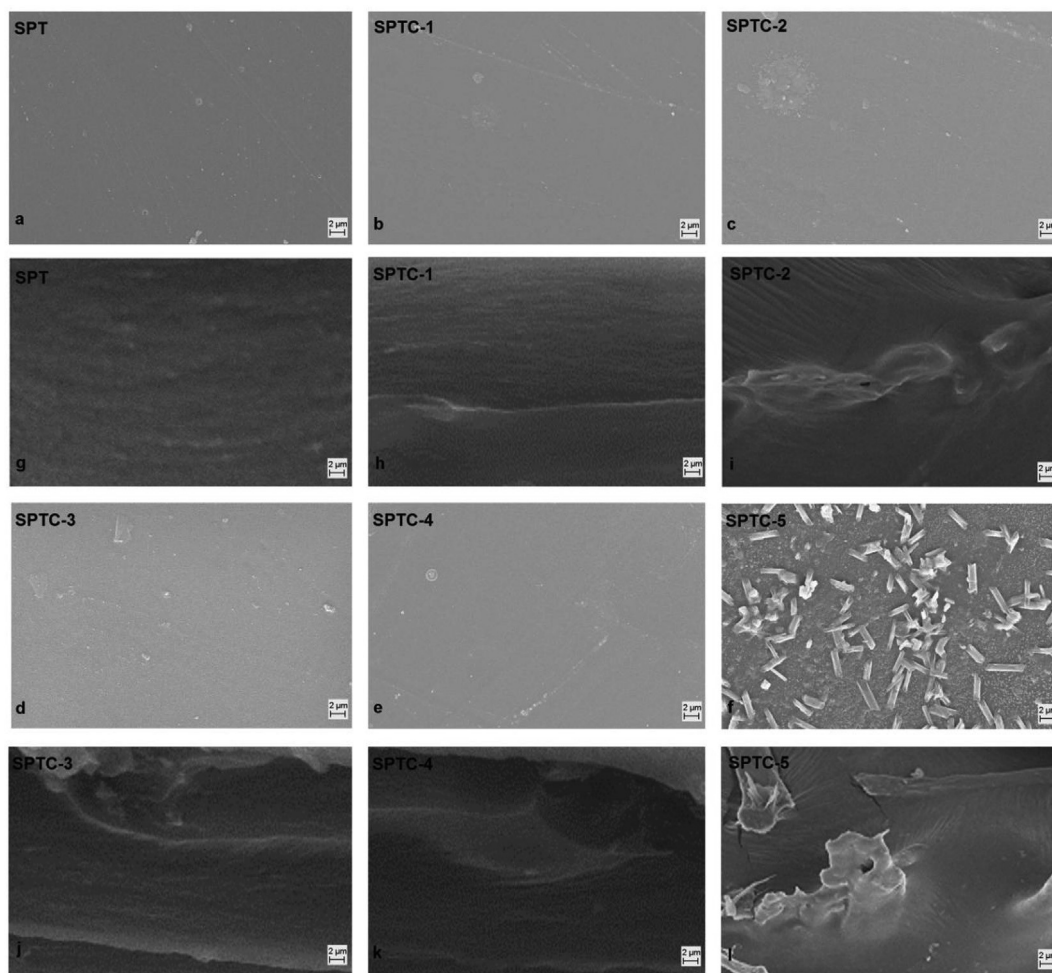


**Fig. 9.** SEM micrographs of crosslinked sulfonated PVA (SPT) and its sulfonated  $\beta$ -CD incorporated composite membranes (SPTC-1 to SPTC-5): surface views (a–f) and cross-sectional views (g–l).

responsible for the enlargement of ionic channels and thereby limits the mechanical strength, dimensional stability and thermal stability of the membranes. This in turn increases the free-volume in the membrane matrix and provides the space for the transport of protons, which helps to increase the proton conductivity of the membranes. Therefore, it is important to control the optimum swelling ratio of the membranes. From the swelling ratio data, it is observed that upon incorporating the sulfonated  $\beta$ -CD and increase of its mass% in SPT membrane, the swelling ratio of length and thickness was increased respectively from 33.2 to 43% and 29.9 to 39.2% at 80 °C. The resulting swelling ratios are adequate and useful for the overall improvement of membrane applications. This is mainly due to an establishment of dense network structure between the TGDMP crosslinker and sulfonated  $\beta$ -CD in PVA matrix.

### 3.9. Ion exchange capacity

The IEC is an important parameter for the evaluation of PEMs as it directly influences on the water uptake and proton conductivity. The IEC values of the crosslinked sulfonated PVA and its composite membranes determined by a back titration method are included in Table 3, and results are also presented in Fig. 13. From the data, it is observed that IEC values were increased almost linearly with increasing the mass% of sulfonated  $\beta$ -CD. These are in good agreement with the water uptake data.

The introduction of pendant  $-\text{SO}_3\text{H}$  groups in the polymer chains plays an important role in enhancing the ion exchange capacity of the membrane. The introduction of  $-\text{SO}_3\text{H}$  groups beyond certain mass% in the membrane decreases the membranes dimensional stability. On the other hand, the increased  $-\text{SO}_3\text{H}$  groups in the polymer backbone restrict the segmental motion of the polymer chains and thus imparts rigidity to the polymer chains. This in turn decreases the water uptake and thereby restricts the transport of protons across the membrane. Therefore, it is essential to optimize the degree of sulfonation to retain both dimensional stability and ion exchange capacity. Understanding this, we have optimized the degree of sulfonation in PVA and that was found to be 54%.

### 3.10. Proton conductivity

Proton conductivity is another important parameter being used to understand the propensity of membrane to transport protons. The proton conductivity of membrane in hydrated state is greatly dependent on the content of water, dissociation of immobile sulfonic acid groups and mobile protons within the swollen membrane matrix. Thus, measurement of proton conductivity was systematically carried out with respect to mass% of sulfonated  $\beta$ -CD in hydrated state (100% relative humidity) at different temperatures, and the results are presented in Table 3 as well as in Figs. 14

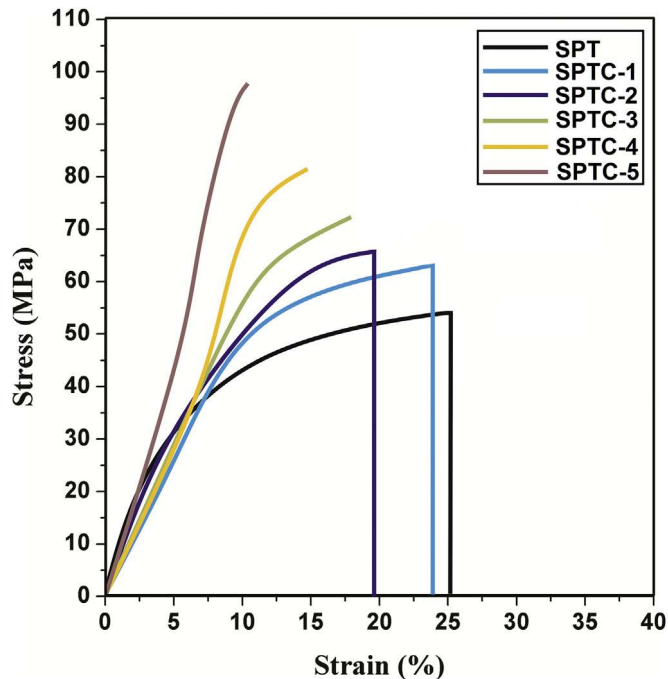


Fig. 10. Stress and strain curves of crosslinked sulfonated PVA (SPT) and its sulfonated  $\beta$ -CD incorporated composite membranes (SPTC-1 to SPTC-5).

Table 2

The oxidative and hydrolytic properties of TGDMP crosslinked sulfonated PVA and its composite membranes.

Membranes	Oxidative stability			Hydrolytic stability	
	RW%	T(h)	IEC loss (%)	RW%	IEC loss (%)
SPT	96.4	>22	6.2	94.7	6.9
SPTC-1	94.2	>17	8.6	94.9	8.2
SPTC-2	94.0	>17	9.3	94.7	8.5
SPTC-3	93.6	>17	9.5	94.3	8.9
SPTC-4	93.4	>17	9.8	93.8	9.2
SPTC-5	93.0	>17	9.8	93.6	9.6

RW%: Percent of the remaining weight.

and 15. In crosslinked membranes, the crosslinking segments usually create rigidity in the membrane matrix, and thereby it leads to a tortuous pathway for transport of water and protons, which in turn suppress the proton conductivity of the membranes. On the contrary, carboxylic groups present in the TGDMP crosslinker help to increase the water uptake, and thereby increases the proton conductivity of membranes. From the data, it is also observed that proton conductivity of the crosslinked sulfonated PVA membrane was greatly enhanced with increasing the mass% of sulfonated  $\beta$ -CD. This is mainly due to increased reactive sulfonic acid groups in the membrane matrix and thereby the distance between the sulfonic acid groups was reduced. This in turn becomes responsible for the overall increase of proton conductivity. Similarly, proton conductivity of the membranes was increased with increasing the temperature. This indicates that temperature plays a significant role in enhancing the kinetics of protons in the membrane matrix and thereby the proton conductivity was greatly increased. As similar to IEC results, membranes particularly incorporated with 16 and 20 mass% sulfonated  $\beta$ -CD demonstrated excellent proton conductivity at 80 °C. This is very important in the light of the existing fuel cell technology, which generally works at 80 °C.

In view of the dependency of proton conductivity ( $S$ ) on the

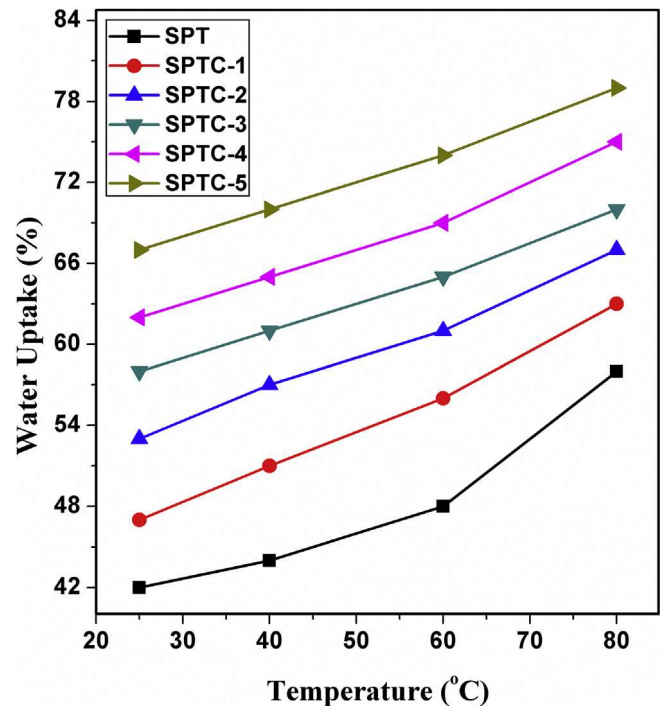


Fig. 11. Water uptake of crosslinked sulfonated PVA (SPT) and its sulfonated  $\beta$ -CD incorporated composite membranes (SPTC-1 to SPTC-5).

temperature, it is prompted to calculate the activation energies for all the resulting membranes using the Arrhenius type equation [37]:

$$S = A e^{-E_a/RT} \quad (7)$$

where  $S$  is the proton conductivity (S/cm),  $E_a$  is the activation energy (kJ/mol) and other terms are as usual.

Arrhenius plots of  $\log S$  versus  $1/T$  are shown in Fig. 16 for the temperature dependence of proton conductivity. From the least-squares fits of these linear plots, the activation energies were calculated. In all the cases, a linear behavior was observed, suggesting that proton conductivity follows an Arrhenius trend. The resulting activation energy values are presented in Table 3. The values of  $E_a$  ranged between 10.33 and 16.54 kJ/mol, which are lower than that of Nafion<sup>®</sup> 117 membrane (20 kJ/mol) [38]. This suggests that the developed membranes consumed minimum energy for the transport of protons across the membranes. This is mainly because of increased ion exchange capacity owing to the presence of large number of  $-\text{SO}_3\text{H}$  groups contributed from both sulfonated PVA and  $\beta$ -CD. Based on these energy values, we conclude that the Grotthus (hopping) mechanism was predominant for the transport of protons across the membrane.

### 3.11. Fuel cell performance and durability

The fuel cell performance of the developed membranes was investigated using a single cell MEA and resulting values are presented in Fig. 17. Among the membranes developed, the SPT membrane exhibited relatively lower open circuit voltage (OCV) value of 0.746 V with a current density of 0.58 A/cm<sup>2</sup>. In contrast to this, the composite membranes having 20 mass% of sulfonated  $\beta$ -cyclodextrin demonstrated the highest power density of 0.38 W/cm<sup>2</sup> at 0.61 A/cm<sup>2</sup> with an OCV value of 0.848 V. Similarly, membrane containing 16 mass% of sulfonated  $\beta$ -cyclodextrin showed

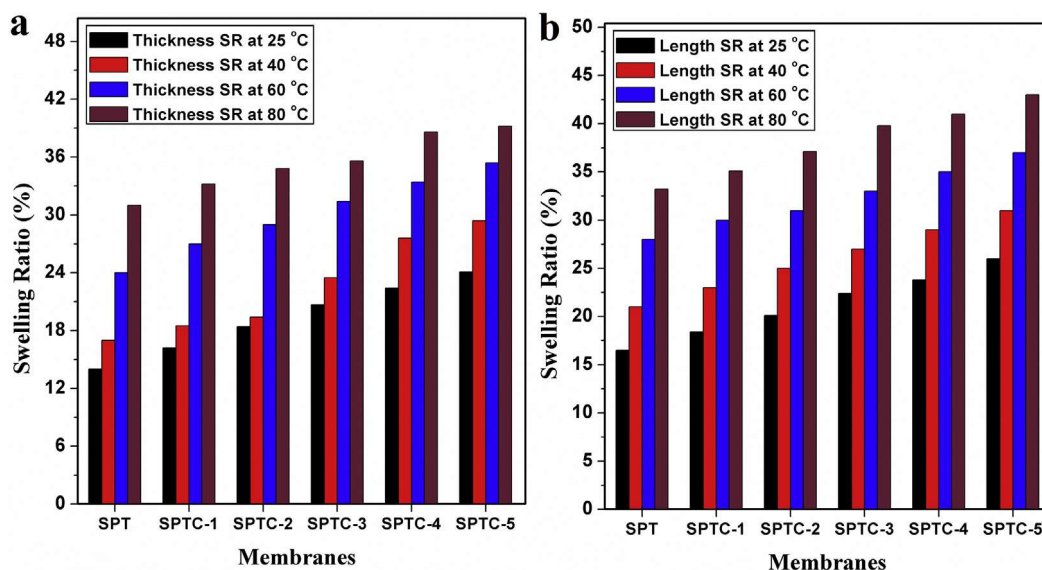


Fig. 12. Swelling ratio (a) length and (b) thickness of crosslinked sulfonated PVA (SPT) and its sulfonated  $\beta$ -CD incorporated composite membranes (SPTC-1 to SPTC-5).

Table 3

Water uptake, swelling ratio, IEC, proton conductivity and activation energy of TGDMP crosslinked sulfonated PVA and its composite membranes.

Membranes	Water uptake (%)		Swelling ratio (%) Length Thickness				IEC (meq/g)	Proton conductivity (S/cm)		$E_a$ (kJ/mol)
	25 °C	80 °C	25 °C	80 °C	25 °C	80 °C		25 °C	80 °C	
SPT	42	58	16.5	33.2	14.1	29.9	1.35	0.015	0.042	16.52
SPTC-1	47	63	18.4	35.1	16.2	33.2	1.40	0.021	0.060	16.71
SPTC-2	53	67	20.1	37.1	18.4	34.8	1.61	0.039	0.071	12.60
SPTC-3	58	70	22.4	39.8	20.7	35.6	1.81	0.045	0.088	10.82
SPTC-4	62	75	23.8	41.0	22.4	38.6	2.10	0.059	0.121	11.11
SPTC-5	67	79	26.0	43.0	24.1	39.2	2.55	0.073	0.143	10.33
Nafion® 117 <sup>a</sup>	22	38	10.6	17.2	–	–	0.90	0.080	0.100	20.00

<sup>a</sup> Data of Nafion® 117 are collected from Refs. [38,39].

the power density of  $0.34 \text{ W/cm}^2$  at  $0.53 \text{ A/cm}^2$  with an OCV value of  $0.824 \text{ V}$ . These values are much superior to the existing commercial Nafion® 117 membrane (OCV of  $0.56 \text{ V}$  with a power density of  $9 \text{ mW/cm}^2$ ) [40]. The highest power density observed in SPTC-4 and SPTC-5 membranes is mainly due to higher charge density created in the crosslinked PVA membrane by the incorporation of an optimum mass% of sulfonated  $\beta$ -cyclodextrin. This is well supported from the proton conductivity data. It is further concluded that the overall electrochemical results of the composite membranes demonstrated an excellent performance due to the presence of higher mass% of sulfonated  $\beta$ -cyclodextrin in the crosslinked polymer network, which greatly enhanced the exchange of protons among the sulfonic groups in the polymer matrix.

To assess the durability, only SPTC-4 and SPTC-5 membranes were selected and subjected to a short term stability study at a fixed current density of  $0.2 \text{ A/cm}^2$  for 100 h, and the results thus obtained are presented in Fig. 18. It is observed that the cell voltage of SPTC-4 was marginally decreased from  $0.620$  to  $0.604 \text{ V}$  for 100 h. But no significant change in the cell voltage was noticed in SPTC-5 membrane. This clearly suggests that both TGDMP and sulfonated  $\beta$ -CD greatly contributed for enhancing the overall durability performance of the membranes.

### 3.12. Comparative study of fuel cell performance of PVA based membranes

In order to compare the fuel cell performance of the developed

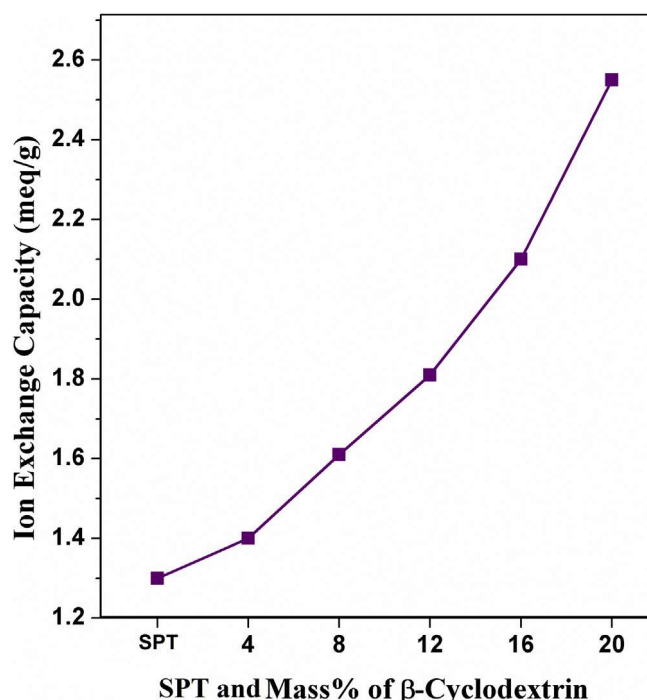


Fig. 13. Ion exchange capacity of crosslinked sulfonated PVA (SPT) and its sulfonated  $\beta$ -CD incorporated composite membranes (SPTC-1 to SPTC-5).

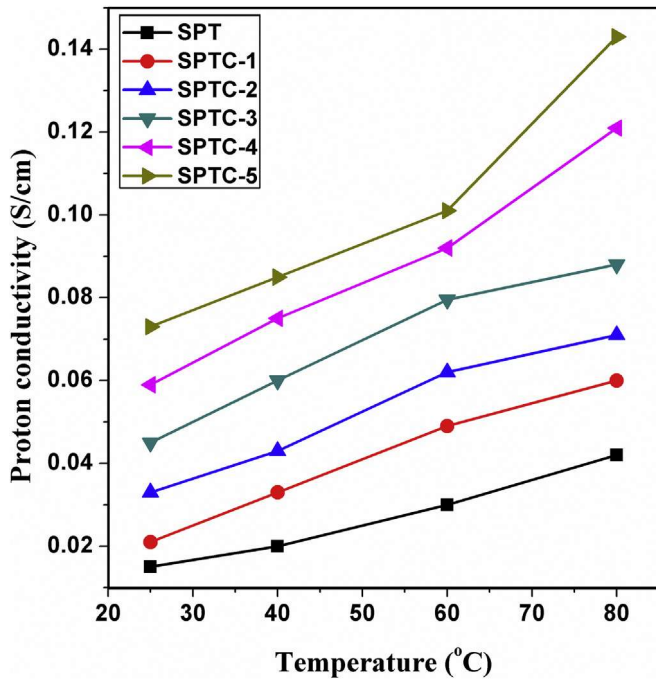


Fig. 14. Temperature dependence proton conductivity of crosslinked sulfonated PVA (SPT) and its sulfonated  $\beta$ -CD incorporated composite membranes (SPTC-1 to SPTC-5) at 100% relative humidity.

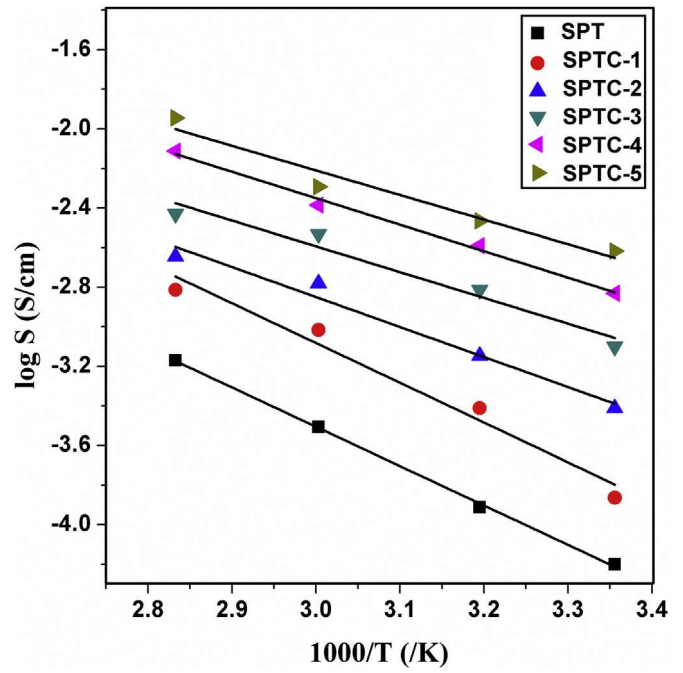


Fig. 16. Arrhenius plots of proton conductivity for crosslinked sulfonated PVA (SPT) and its sulfonated  $\beta$ -CD incorporated composite membranes (SPTC-1 to SPTC-5).

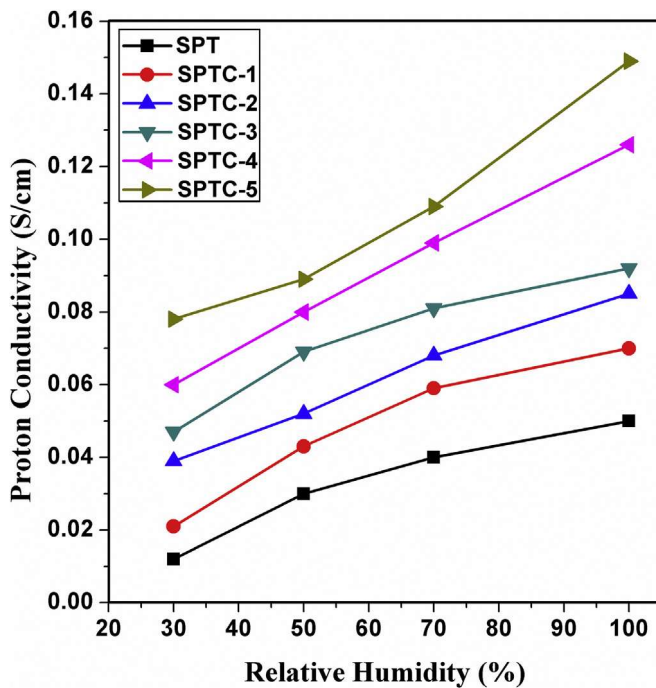


Fig. 15. Humidity dependence proton conductivity of crosslinked sulfonated PVA (SPT) and its sulfonated  $\beta$ -CD incorporated composite membranes (SPTC-1 to SPTC-5) at 80 °C.

membranes with the PVA based inorganic-organic hybrid membranes reported in the literature, we have summarized the data of proton conductivity, power density, ion exchange capacity including the tensile strength and thickness of the membranes in Table 4. Among the membranes reported here, PVA/PHB [16] and Nafion/PVA [48] membranes demonstrated excellent power

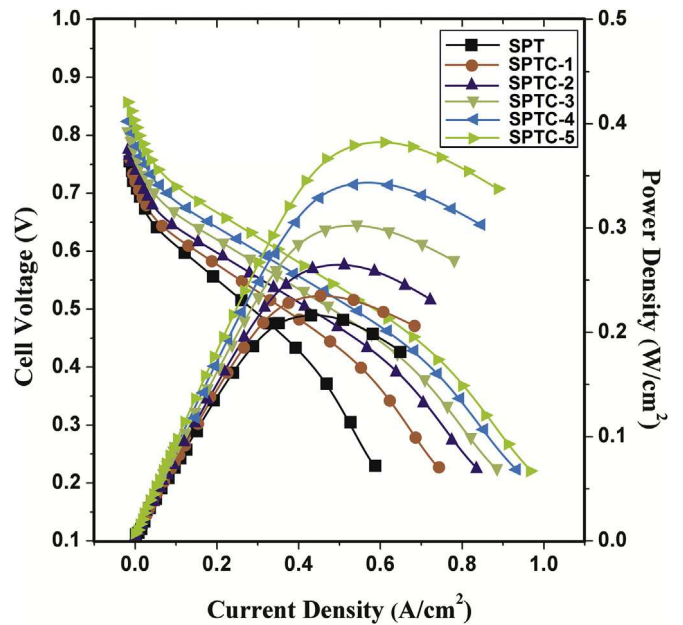


Fig. 17. Polarization and power density curves of crosslinked sulfonated PVA (SPT) and its sulfonated  $\beta$ -CD incorporated composite membranes (SPTC-1 to SPTC-5).

density of 620 and 477  $\text{mW}/\text{cm}^2$ , respectively. However, the other properties like proton conductivity, ion exchange capacity and tensile strength of these two membranes are much lower than that of the membranes developed here. Similarly, the proton conductivity of PVA/ $\text{H}_3\text{BO}_3$ / $\text{BPO}_4$  [49] and SPVA/ODPA/epoxy [26] membranes is higher, but their power density and tensile strength are much lower as compared to the membranes developed. The other membranes presented in Table 4 are no way comparable to the membranes developed in the present study. Thus, it is concluded that the developed membranes are much superior to the PVA based

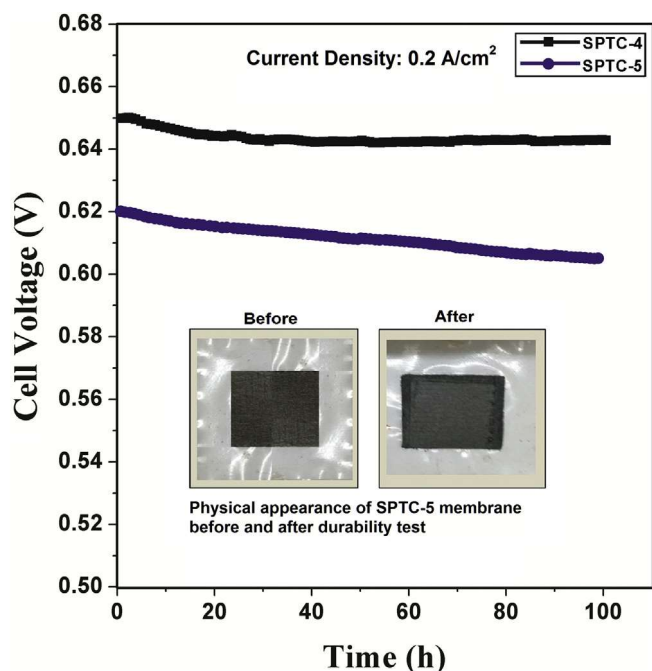


Fig. 18. Durability results of SPTC-4 and SPTC-5 membranes at current density of 0.2 A/cm<sup>2</sup>.

inorganic-organic hybrid membranes reported in the literature.

PVA: poly(vinyl alcohol); SPVA: sulfonated poly(vinyl alcohol); PHB: polyhydroxybutyrate; PVP: poly(vinyl pyrrolidone); BaZrO<sub>3</sub>: barium zirconate; HFA: hexafluoroglutaric acid; BASANa: benzenesulfonic acid sodium salt; GA: glutaraldehyde; PAMPS: poly(2-acrylamido-2-methyl-1-propanesulfonic acid); Tn: terephthalaldehyde; PVACO: poly(vinyl alcohol-co-vinyl acetate-co-itaconic acid); PMA: phosphomolybdic acid; SGO: sulfonated graphene oxide; SBA-15-propyl-SO<sub>3</sub>H: sulfonated nanoporous silica; ODADS: 4,4'-diaminodiphenylether-2,2'-disulfonic acid; ODPa:

4,4'-oxydiphthalic anhydride; PVA-*b*-PSSA: poly(vinyl alcohol-*b*-styrene sulfonic acid); C-SPAEEKS: crosslinked sulfonated poly(arylene ether ketone sulfone); SPEEK: sulfonated poly(ether ether ketone); MMT: montmorillonite; PSSA: poly(styrene sulfonic acid); AMPS: 2-methyl-1-propanesulfonic acid; PES: poly(ether sulfone); PWA: phosphotungstic acid; PAM: polyacrylamide; CsPMA: cesium salts of phosphomolybdic acid; Si-PWA: silica immobilized phosphotungstic acid; HPW: phosphotungstic acid; CNT: carbon nanotube; PDDA: poly(diallyldimethylammonium chloride); TEOS: tetraethyl ortosilicate.

#### 4. Conclusions

In this study, the composite membranes were successfully developed by the incorporation of sulfonated  $\beta$ -CD into TGDMP crosslinked sulfonated PVA. Being TGDMP as a crosslinker, it enhanced both hydrophilicity and proton conductivity of the PVA membrane owing to the presence of carboxylic groups in TGDMP. Further to enhance the proton conductivity of the SPT membrane, the sulfonated  $\beta$ -CD was incorporated in different mass ratios. The presence of large number of sulfonic groups in  $\beta$ -CD as well as in crosslinked sulfonated PVA, significantly enhanced the proton conductivity of the composite membranes. In addition, the hydrophobic segment of PVA chain and inorganic crosslinker (TGDMP) increased the dimensional stability of the composite membranes. At 80 °C, the water uptake and swelling ratio of the composite membranes were increased from 63 to 79% and 35.1 to 43% with increasing the mass% of sulfonated  $\beta$ -CD. Similarly, IEC values were found to increase from 1.40 to 2.55 meq/g with increasing the sulfonated  $\beta$ -CD from 4 to 20%. The experimental results suggest that the membrane containing 20 mass% of sulfonated  $\beta$ -CD exhibited the highest proton conductivity of 0.73 S/cm at 25 °C, and 0.143 at 80 °C. The results revealed that the proton conductivity was mainly dependent on the chemical structure of polymer matrix, crosslinker and  $\beta$ -CD. The results of fuel cell performance also indicate that the composite membranes demonstrated much superior power density as compared to TGDMP crosslinked sulfonated PVA membrane (SPT). On the whole, the combination of

Table 4  
Comparative study of fuel cell performance of PVA based membranes reported in the literature.

Membranes	Thickness ( $\mu$ m)	TS (MPa)	IEC (meq/g)	S/ $^{\circ}$ C (mS/cm)	P <sub>max</sub> / $^{\circ}$ C (mW/cm <sup>2</sup> )	Refs.
SPVA/TGDMP/ $\beta$ -CD (16%)	85	81	2.10	121/80	340/80	#
SPVA/TGDMP/ $\beta$ -CD (20%)	83	97	2.55	143/80	380/80	#
PVA/PHB	50	35	1.12	86/80	620/80	[16]
PVA/PVP/BaZrO <sub>3</sub>	NA	101	NA	60.1/70	29/70	[17]
PVA/HFA/BASANa/GA	100–250	18	1.16	62.7/60	NA	[18]
PVA/PAMPS/Tn	100–300	NA	1.63	120/25	NA	[20]
PVACO/PMA	100	32	NA	2.6/NA	NA	[21]
PVA/SGO	~150	68	0.92	50/80	16.15/30	[22]
PVA/GA/SBA-15-propyl-SO <sub>3</sub> H	250–300	NA	NA	6/25	NA	[23]
PVA/ODADS	120	NA	NA	16/30	NA	[25]
SPVA/ODPA/epoxy	100	11	2.40	218/70	81/70	[26]
PVA/PAMPS/1,2,4-triazole/GA	90 and 150	NA	1.62	2/150	NA	[27]
SPEEK/SPVA	NA	NA	1.10	34/80	23.32/80	[28]
PVA/AMPS	95	16	0.31	12.5/25	2.4/NA	[29]
PVA/MMT/PSSA	100–200	NA	NA	12/70	20/25	[38]
PVA- <i>b</i> -PSSA/GA	50–70	15	1.00	16.8/60	31.2/60	[41]
C-SPAEEKS/SPVA	50–100	36	1.75	85/80	NA	[42]
PVA/PES/PWA	100–120	37	0.52	0.74/NA	112/80	[43]
PVA/PAM/GA/CsPMA	250	0.65	0.73	3.7/25	37/25	[44]
PVA/Si-PWA	80–100	92	0.90	10.5/50	29.6/35	[45]
PVA/HPW-CNT-PDDA	NA	NA	3.49	5.2/30	16/60	[46]
SPEEK/PVA/TEOS	NA	48	2.02	85/80	336/80	[47]
Nafion/PVA	19	35	NA	57/80	477/80	[48]
PVA/H <sub>3</sub> BO <sub>3</sub> /BPO <sub>4</sub>	NA	72	1.36	370/80	0.48/80	[49]

#: Present work; NA: Not available; TS: Tensile stress; S/ $^{\circ}$ C: Proton conductivity/temperature; OCV: Open circuit voltage; P<sub>max</sub>/ $^{\circ}$ C: Power density/temperature.

thermal stability, dimensional stability, proton conductivity and fuel cell performance makes the composite membranes particularly SPTC-4 and SPTC-5 as potential candidates for fuel cell applications.

## Acknowledgements

The authors (Balappa B. Munavalli and Satishkumar R. Naik) thank the UGC, New Delhi, for awarding the RFSMS fellowships to carry out the research work. The authors wish to thank the Department of Science & Technology, New Delhi, for providing the financial support under DST-PURSE-Phase-II program [Grant No. SR/PURSE PHASE-2/13(G)]. The authors remain grateful to Dr. Fred J. Davis, Professor, Department of Chemistry, University of Reading, Reading, UK, for doing the language corrections in the manuscript.

## References

- [1] X. Luo, J. Wang, M. Dooner, J. Clarke, Overview of current development in electrical energy storage technologies and the application potential in power system operation, *Appl. Energy* 137 (2015) 511–536.
- [2] H. Chen, T.N. Cong, W. Yang, C. Tan, Y. Li, Y. Ding, Progress in electrical energy storage system: a critical review, *Prog. Nat. Sci.* 19 (2009) 291–312.
- [3] M.Y. Kariduraganavar, B.B. Munavalli, A.I. Torvi, Proton conducting polymer electrolytes for fuel cells via electrospinning technique, in: A. Mohammad Inamuddin, A.M. Asiri (Eds.), *Organic-inorganic Composite Polymer Electrolyte Membranes*, Springer International Publishing, 2017, pp. 421–458.
- [4] F.A. Zakil, S.K. Kamarudin, S. Basri, Modified Nafion membranes for direct alcohol fuel cells: an overview, *Renew. Sustain. Energy Rev.* 65 (2016) 841–852.
- [5] H. Lade, V. Kumar, G. Arthanareeswaran, A.F. Ismail, Sulfonated poly(arylene ether sulfone) nanocomposite electrolyte membrane for fuel cell applications: a review, *Int. J. Hydrogen Energy* 42 (2017) 1063–1074.
- [6] B. Munavalli, A. Torvi, M. Kariduraganavar, A facile route for the preparation of proton exchange membranes using sulfonated side chain graphite oxides and crosslinked sodium alginate for fuel cell, *Polymer* 142 (2018) 293–309.
- [7] K. Miyatake, H. Furuya, M. Tanaka, M. Watanabe, Durability of sulfonated polyimide membrane in humidity cycling for fuel cell applications, *J. Power Sources* 204 (2012) 74–78.
- [8] J. Chen, J. Wu, C. Lee, M. Tsai, K. Chen, Novel polyimides containing benzimidazole for temperature proton exchange membrane fuel, *J. Membr. Sci.* 483 (2015) 144–154.
- [9] Y. Özdemir, N. Özkan, Y. Devrim, Fabrication and characterization of cross-linked polybenzimidazole based membranes for high temperature PEM fuel cells, *Electrochim. Acta* 245 (2017) 1–3.
- [10] Y. Jeong, J. Jung, E. Choi, S. Han, A.I. Begley, S.J. Yoo, J.H. Jang, H. Kim, S.W. Nam, K. Lee, J.Y. Kim, Colorimetric determination of phosphoric acid leakage for phosphoric acid-doped polybenzimidazole membrane fuel cell applications, *J. Power Sources* 299 (2015) 480–484.
- [11] S. Kwon, B. Lee, T. Kim, High performance blend membranes based on densely sulfonated poly(fluorenyl ether sulfone) block copolymer and imidazolium-functionalized poly(ether sulfone), *Int. J. Hydrogen Energy* 42 (2017) 20176–20186.
- [12] J.R. Rowlett, V. Lilavivat, A.T. Shaver, Y. Chen, A. Daryaei, H. Xu, C. Mittelsteadt, S. Shimpalee, J.S. Riffle, J.E. McGrath, Multiblock poly(arylene ether nitrile) disulfonated poly(arylene ether sulfone) copolymers for proton exchange membranes: Part 2 electrochemical and H<sub>2</sub>/Air fuel cell analysis, *Polymer* 122 (2017) 296–302.
- [13] W. Guo, X. Li, H. Wang, J. Pang, G. Wang, Z. Jiang, S. Zhang, Synthesis of branched sulfonated poly(aryl ether ketone) copolymers and their proton exchange membrane properties, *J. Membr. Sci.* 444 (2013) 259–267.
- [14] L. Xu, J. Xu, M. Liu, H. Han, H. Ni, L. Ma, Z. Wang, Fabrication of sulfonated poly(aryl ether ketone sulfone) membranes blended with phosphotungstic acid and microporous poly(vinylidene fluoride) as a depository for direct-methanol fuel cells, *Int. J. Hydrogen Energy* 40 (2015) 7182–7191.
- [15] Y. Li, H. Wang, Q. Wu, X. Xu, S. Lu, Y. Xiang, A PVA-based composite membrane with immobilized phosphotungstic acid molecules for direct methanol fuel cells, *Electrochim. Acta* 224 (2017) 369–377.
- [16] M.M. El-Toony, E.E. Abdel-Hady, N.A. El-Kelsh, Casting of poly hydroxybutyrate/PVA membranes for proton exchange fuel cells, *Electrochim. Acta* 150 (2014) 290–297.
- [17] A.M. Attaran, M. Javanbakht, K. Hooshiyari, M. Enhessari, New proton conducting nanocomposite membranes based on poly vinylalcohol/poly vinyl pyrrolidone/BaZrO<sub>3</sub> for proton exchange membrane fuel cells, *Solid State Ionics* 269 (2015) 98–105.
- [18] C. Liu, C. Dai, C. Chao, S. Chang, Novel proton exchange membrane based on crosslinked PVA for direct methanol fuel cells, *J. Power Sources* 249 (2014) 285–298.
- [19] S.S. Madaeni, S. Amirinejad, M. Amirinejad, Phosphotungstic acid doped PVA/poly(ether sulfone) blend composite membranes for direct methanol fuel cells, *J. Membr. Sci.* 380 (2011) 132–137.
- [20] J. Qiao, T. Hamaya, T. Okada, Chemically modified PVA-poly(2-acrylamido-2-methyl-1-propanesulfonic acid) as a novel proton-conducting fuel cell membrane, *Chem. Mater.* 17 (2005) 2413–2421.
- [21] A. Anis, A.K. Banthia, S. Bandyopadhyay, Synthesis and characterization of polyvinyl alcohol copolymer/phosphomolybdic acid-based crosslinked composite polymer electrolyte membranes, *J. Power Sources* 179 (2008) 69–80.
- [22] H. Beydaghi, M. Javanbakht, E. Kowsari, Synthesis and characterization of PVA/sulfonated graphene oxide nanocomposite membranes for use in proton exchange membrane fuel cells (PEMFCs), *Ind. Eng. Chem. Res.* 53 (2014) 16621–16632.
- [23] H. Beydaghi, M. Javanbakht, A. Badiei, Cross-linked PVA/sulfonated nanoporous silica hybrid membranes for proton exchange membrane fuel cell, *J. Nanostruct. Chem.* 97 (2014) 1–9.
- [24] R. Boonpoo-nga, M. Siring, P. Nasomjai, S. Martwiset, Electrospun fibres from polyvinyl alcohol, poly(styrenesulphonic acid-co-maleic acid), and imidazole for proton exchange membranes, *Sci. Asia* 40 (2014) 232–237.
- [25] M.S. Boroglu, S. Cavus, I. Boz, A. Ata, Synthesis and characterization of PVA proton exchange membranes modified with 4,4-diaminodiphenylether-2,2-disulfonic acid, *Express Polym. Lett.* 5 (2011) 470–478.
- [26] C. Tseng, Y. Ye, K. Kao, J. Joseph, W. Shen, J. Rick, B. Hwang, Interpenetrating network-forming sulfonated PVA proton exchange membranes for direct methanol fuel cell applications, *Int. J. Hydrogen Energy* 36 (2011) 11936–11945.
- [27] M. Erkartal, A. Aslan, U. Erkilic, S. Dadi, O. Yazaydin, H. Usta, U. Sen, Anhydrous proton conducting poly(vinyl alcohol) (PVA)/poly(2-acrylamido-2-methylpropane sulfonic acid) (PAMPS)/1,2,4-triazole composite membrane, *Int. J. Hydrogen Energy* 41 (2016) 1–10.
- [28] T. Yang, Composite membrane of sulfonated poly(ether ether ketone) and sulfated poly(vinyl alcohol) for use in direct methanol fuel cells, *J. Membr. Sci.* 342 (2009) 221–226.
- [29] M. Higa, K. Hatemura, M. Sugita, S.-i. Maesowa, M. Nishimura, N. Endo, Performance of passive direct methanol fuel cell with poly(vinyl alcohol)-based polymer electrolyte membranes, *Int. J. Hydrogen Energy* 37 (2012) 6292–6301.
- [30] R. Li, C. Liu, J. Ma, Y. Yang, H. Wu, Effect of org-titanium phosphonate on the properties of chitosan films, *Polym. Bull.* 67 (2011) 77–89.
- [31] H.G. Premakshi, A.M. Sajjan, M.Y. Kariduraganavar, Development of pervaporation membranes using chitosan and titanium glycine-N,N-dimethylphosphonate for dehydration of isopropanol, *J. Mater. Chem. A* 3 (2015) 3952–3961.
- [32] S. Brück, C. Krause, R. Turrisi, L. Beverina, S. Wilken, W. Saak, A. Lützen, H. Borchert, M. Schiek, J. Parisi, Structure–property relationship of anilino-squaraines in organic solar cells, *Phys. Chem. Chem. Phys.* 16 (2014) 1067–1077.
- [33] H. Jung, J.W. Kim, Role of the glass transition temperature of Nafion 117 membrane in the preparation of the membrane electrode assembly in a direct methanol fuel cell (DMFC), *Int. J. Hydrogen Energy* 37 (2012) 12580–12585.
- [34] H.W. Starkweather, Crystallinity in perfluorosulfonic acid ionomers and related polymers, *Macromolecules* 15 (1982) 320–323.
- [35] S. Feng, K. Shen, Y. Wang, J. Pang, Z. Jiang, Concentrated sulfonated poly(ether sulfone)s as proton exchange membranes, *J. Power Sources* 224 (2013) 42–49.
- [36] J. Healy, C. Heyden, T. Xie, K. Olson, R. Waldo, M. Brundage, H. Gasteiger, J. Abbott, Aspects of the chemical degradation of PFSA ionomers used in PEM fuel cells, *Fuel Cell* 5 (2004) 302–308.
- [37] A.M. Sajjan, B.K. Jeevan Kumar, A.A. Kittur, M.Y. Kariduraganavar, Novel approach for the development of pervaporation membranes using sodium alginate and chitosan-wrapped multiwalled carbon nanotubes for the dehydration of isopropanol, *J. Membr. Sci.* 425–426 (2013) 77–88.
- [38] C.-C. Yang, Fabrication and characterization of poly(vinyl alcohol)/montmorillonite/poly(styrene sulfonic acid) proton-conducting composite membranes for direct methanol fuel cells, *Int. J. Hydrogen Energy* 36 (2011) 4419–4431.
- [39] L. Zhang, G. Zhang, C. Zhao, H. Jiang, J. Wang, D. Xu, Y. Zhang, K. Shao, Z. Liu, W. Ma, H. Li, M. Li, S. Wang, H. Na, Cross-linked tri-side chains poly(arylene ether ketone)s containing pendant alkyl sulfonic acid groups for proton exchange membranes, *J. Power Sources* 201 (2012) 142–150.
- [40] J. Tsai, J. Kuo, C. Chen, Synthesis and properties of novel HMS-based sulfonated poly(arylene ether sulfone)/silica nano-composite membranes for DMFC applications, *J. Power Sources* 174 (2007) 103–113.
- [41] M. Higa, S. Feng, N. Endo, Y. Kakihana, Characteristics and direct methanol fuel cell performance of polymer electrolyte membranes prepared from poly(vinyl alcohol-b-styrene sulfonic acid), *Electrochim. Acta* 153 (2015) 83–89.
- [42] J. Xu, H. Ni, S. Wang, Z. Wang, H. Zhang, Direct polymerization of a novel sulfonated poly(arylene ether ketone sulfone)/sulfonated poly(vinylalcohol) crosslinked membrane for direct methanol fuel cell applications, *J. Membr. Sci.* 492 (2015) 505–517.
- [43] S.S. Madaeni, S. Amirinejad, M. Amirinejad, Phosphotungstic acid doped poly(vinyl alcohol)/poly(ether sulfone) blend composite membranes for direct methanol fuel cells, *J. Membr. Sci.* 380 (2011) 132–137.
- [44] M. Helen, B. Viswanathan, S.S. Murthy, Poly(vinyl alcohol)-polyacrylamide blends with cesium salts of heteropolyacid as a polymer electrolyte for direct methanol fuel cell applications, *J. Appl. Polym. Sci.* 116 (2010) 3437–3447.
- [45] J. Pandey, F.Q. Mir, A. Shukla, Synthesis of silica immobilized phosphotungstic

- acid (Si-PWA)-poly(vinyl alcohol) (PVA) composite ion-exchange membrane for direct methanol fuel cell, *Int. J. Hydrogen Energy* 39 (2014) 9473–9481.
- [46] Y. Li, H. Wang, Q. Wu, X. Xu, S. Lu, Y. Xiang, A poly(vinyl alcohol)-based composite membrane with immobilized phosphotungstic acid molecules for direct methanol fuel cells, *Electrochim. Acta* 224 (2017) 369–377.
- [47] A. Sahin, The development of Speek/Pva/Teos blend membrane for proton exchange membrane fuel cells, *Electrochim. Acta* 271 (2018) 127–136.
- [48] S. Molla, V. Compan, E. Gimenez, A. Blazquez, I. Urdanpilleta, Novel ultrathin composite membranes of Nafion/PVA for PEMFCs, *Int. J. Hydrogen Energy* 36 (2011) 9886–9895.
- [49] A. Sahin, I. Ar, Synthesis, characterization and fuel cell performance tests of boric acid and boron phosphate doped, sulphonated and phosphonated poly(vinyl alcohol) based composite membranes, *J. Power Sources* 288 (2015) 426–433.

## Nomenclature

PEM: proton exchange membrane  
 PEMFC: proton exchange membrane fuel cell  
 PVA: poly(vinyl alcohol)

TGDMP: titanium glycine-*N,N*-dimethylphosphonate  
 $\beta$ -CD:  $\beta$ -cyclodextrin  
 WU: water uptake  
 SR: swelling ratio  
 $W_S$ : weight of the membrane sample  
 $W_{wet}$  and  $W_{dry}$ : weight of swollen and dry membrane  
 $L_{wet}$  and  $L_{dry}$ : length of swollen and dry membrane  
 RH: relative humidity  
 IEC: ion exchange capacity  
 $M_w$ : molecular weight  
 SEM: scanning electron microscope  
 WAXD: wide angle X-ray diffraction  
 $\Delta V_{NaOH}$ : consumed volume of NaOH solution  
 $C_{NaOH}$ : concentration of NaOH solution  
 DS: degree of sulfonation  
 S: proton conductivity  
 L: distance between electrode  
 A: surface area of the membrane  
 R: resistance  
 MEA: membrane electrode assembly  
 OCV: open circuit voltage